Prone to Supine CT Colonography Registration Using a Landmark and Intensity Composite Method

Thomas E. Hampshire[1], Holger R. Roth[1], Darren J. Boone[2], Greg Slabaugh[3], Steve Halligan[2], and David J. Hawkes[1]

[1] Centre for Medical Image Computing,
University College London, London, WC1E 6BT, UK
thomas.hampshire.09@ucl.ac.uk
[2] Centre for Medical Imaging, University College Hospital, London, UK
[3] Department of Computing, City University, London, UK

Abstract. Matching corresponding location between prone and supine acquisitions for CT colonography (CTC) is essential to verify the existence of a polyp, which can be a difficult task due to the considerable deformations that will often occur to the colon during repositioning of the patient. This can induce error and increase interpretation time. We propose a novel method to automatically establish correspondence between the two acquisitions. A first step segments a set of haustral folds in each view and determines correspondence via a labelling process using a Markov Random Field (MRF) model. We show how the landmark correspondences can be used to non-rigidly transform a 2D source image derived from a conformal mapping process on the 3D endoluminal surface mesh to achieve full surface correspondence between prone and supine views. This can be used to initialise an intensity-based non-rigid B-spline registration method which further increases the accuracy. We demonstrate a statistically significant improvement over the intensity based non-rigid B-spline registration by using the composite method.

Keywords: CT colonography, image registration.

1 Introduction

A number of methods have been proposed to find correspondence between the prone and supine positions. Centreline-based methods extract and align colonic centrelines by stretching and shrinking based on path geometries [12]. These methods are inherently restricted to achieving a registration along a single dimension and do not give any information about the degree of torsion of the colon wall between views. Anatomical landmarks can be used to help align the two datasets by first identifying a stable set of anatomical features, such as the caecum, rectum and flexures [12,6], but stand-alone they do not provide a fine enough registration between views. Voxel-based methods provide a further means of registration [9]. However, these methods rely to varying extents

H. Yoshida, D. Hawkes, M.W. Vannier (Eds.): Abdominal Imaging 2012, LNCS 7601, pp. 1–9, 2012.

upon continuous prone and supine colonic segmentations, free from occlusion by fluid or collapse; a scenario which occurs infrequently in daily practice, despite optimal bowel preparation [10].

Fukano et al. proposed a registration method based on haustral fold matching [1]. A second-order derivative difference filter was used to extract folds; their volume and relative positions along the centreline with respect to a set of locations of high centreline curvature were used to establish correspondence. They reported correct registration of 65.1% of large folds, and 13.3% of small folds; where 9.3% and 32.7% of folds could not be judged.

Zeng et al. combined conformal mapping with feature matching between the prone and supine surfaces [14]. The prone and supine colonic segmentations were mapped onto five rectangle pairs. Correspondences were established using a feature matching method based upon mean curvature. The method relied on accurately determining five matching segments in the prone and supine datasets, which is difficult to achieve and may not be possible in the case of local colonic collapse.

Recently, Hampshire et al. [2] presented a method for generating a set of robust landmark correspondences between the prone and supine CT data using haustral folds. A virtual camera registration is used to create a cost function for matching pairs of folds between the prone and supine acquisitions. A Rotation Minimising Frame (RMF) is swept along the centreline to parametrise the 3D fold position to a 2D vector consisting of centreline distance and angular orientation. Additional fold neighbourhood information in this parametrised space is used to enforce geometric constraints in the form of a pair-wise cost function. The cost functions are incorporated into a MRF model, and a fold labelling assignment is achieved by a Belief Propagation (BP) [13] optimisation process.

Roth et al. [7] provide a full surface registration via a conformal mapping of the prone and supine endoluminal surfaces to 2D cylindrical domains using Ricci flow [3,15], followed by a non-rigid cylindrical intensity based registration using a B-spline method [8] with a sum-of-squared-differences similarity metric based on shape index (SI) [4].

This paper introduces a new composite registration method, first using the sparse positions and displacements of the landmark based registration [2] mapped onto a 2D domain created by performing a conformal mapping using the Ricci flow algorithm [3,15], to construct an underlying function based on multilevel B-splines that can be evaluated at any point to give a transformation from the prone to the supine images. This transformation is further refined by the intensity based registration in [7]. We demonstrate a statistically significant improvement over the previously published methods.

2 B-Spline Approximation

We wish to approximate a smooth function f which relates the (x, y) points in the prone unfolded image, to their (x', y') positions in the supine image over domain $\Omega = (x, y)|0 \leq x < m, 0 \leq y < n$. To do this we use the set of folds $P = \{(x_c, y_c, v_c)\}$ where (x_c, y_c) is a point in Ω and v_c is the value at (x_c, y_c).

We define the mapping in terms of two functions: $x' = X(x, y)$ and $y' = Y(x, y)$. As these functions can be derived simultaneously, we use the notation $v = (x', y') = f(x, y)$. To approximate the data P, we use function f as a uniform bicubic B-spline, defined by control lattice Φ overlaid on domain Ω using the method in [5]. We also assume Φ is an $(m+3)\times(n+3)$ lattice, where m and n are the image dimensions defined in lattice control points. We define ϕ_{ij} as the value of ij-th control point on lattice Ω for $i = -1, 0, ..., m+1$ and $j = -1, 0, ..., n+1$. We can then define the approximation function f:

$$f(x, y) = \sum_{k=0}^{3}\sum_{l=0}^{3} B_k(s)B_l(t)\phi_{(i+k)(j+l)}, \tag{1}$$

where $i = \lfloor x \rfloor - 1, j = \lfloor y \rfloor - 1, s = x - \lfloor x \rfloor$, and $t = y - \lfloor y \rfloor$. B_k and B_l are basis functions:

$$\begin{aligned} B_0(t) &= (1-t)^3/6, \\ B_1(t) &= (3t^3 - 6t^2 + 4)/6, \\ B_2(t) &= (-3t^3 + 3t^2 + 3t + 1)/6, \\ B_3(t) &= (t^3)/6, \end{aligned} \tag{2}$$

where $0 \leq t < 1$. For every point in $P = \{(x_c, y_c, v_c)\}$ a different value ϕ_c of each of the control points ϕ_{ij} is defined:

$$\phi_c = \frac{w_c v_c}{\sum_{a=0}^{3}\sum_{b=0}^{3} w_{ab}^2}, \tag{3}$$

where $w_c = w_{kl} = B_k(s)B_l(t), k = (i+1) - \lfloor x_c \rfloor, l = (j+1) - \lfloor y_c \rfloor, s = x_c - \lfloor x_c \rfloor, t = y_c - \lfloor y_c \rfloor$. Only data points in the 4 x 4 neighbourhood of each control point are taken into consideration. To choose a value for each ϕ_{ij} from the contributions from each point ϕ_c the error $e(\phi_{ij}) = \sum_c (w_c\phi_{ij} - w_c\phi_c)^2$ is minimised by differentiating $e(\phi_{ij})$ with respect to ϕ_{ij} giving:

$$\phi_{ij} = \frac{\sum_c w_c^2 \phi_c}{\sum_c w_c^2}. \tag{4}$$

To allow for a smooth function over the entire domain and more accurate local deformations, a multilevel B-spline approximation is used to generate a hierarchy of control lattices from coarse to fine. A refinement process is used to reduce the sum of these functions into one B-spline function. For each level of control lattice Φ_k we can derive a finer control lattice Φ'_k such that $F(\Phi'_k) = F(\Phi_k)$. We then derive function f_{k+1} by using control lattice Φ_{k+1} to approximate data $P_k = \{(x_c, y_c, \Delta_{k+1}v_c)\}$, where $\Delta_{k+1}v_c = v_c - \sum_{i=0}^{k} f_i(x_c, y_c) = \Delta_k v_c - f_k(x_c, y_c)$, and $\Delta_0 v_c = v_c$. Each function serves to remove the residual error from the coarser lattice at each level. We can now define a progressive control lattice $\Psi_{k+1} = \Phi'_k + \Phi_{k+1}$ from the coarsest to finest levels. We apply this technique to the images created by a conformal mapping [7] of the endoluminal surfaces

of prone and supine images onto a rectangular domain. The sparse set of data points $P = \{(x_c, y_c, v_c)\}$ have their positional information $\{(x_c, y_c)\}$ taken from the positions of haustral folds mapped onto the 2D domain, and the vertical and horizontal displaced positions $\{v_c\}$ of the corresponding positions in the supine image. To allow for a pseudo-continuous function over the y-axis, the image is tripled (figure 1). Due to the true cylindrical nature of the registration problem, there is an ambiguity over the direction of vertical displacement in the 2D images. To create a smooth displacement, the B-spline fitting is repeated and at each iteration the datum P_c with the maximum error between the y component of the estimated and true displacement $e_y = |(F(x_c, y_c) - v_c)_y|$ is adjusted such that $v'_c = v_c + \text{sign}((F(x_c, y_c) - v_c)_y) \cdot y_{max}$ where y_{max} is the size of the image in the y-direction. The image is then shifted in the y-direction so as to minimise v_c and the full multi-level B-spline fitting is repeated to give the final function $F(\Phi)$ with control lattice Φ.

Now for every position in the prone image $P_{prone} = \{(x, y)\} \in \Omega$ we can use the function F to find the corresponding position in the supine image $P_{supine} = \{(x, y)\} \in \Omega$. We can use this transformation alone, or use it as an initialisation to the intensity-based B-spline registration function presented in [7] to create a finer composite registration.

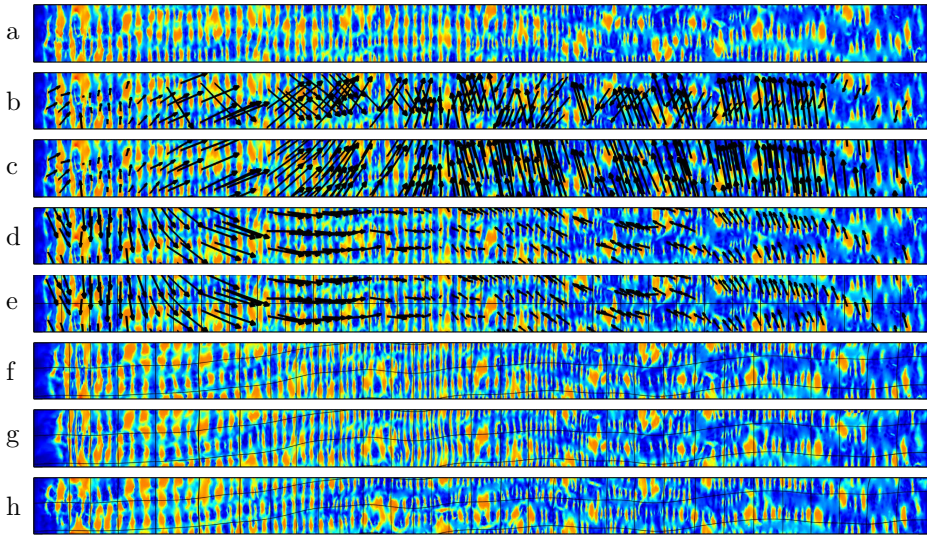

Fig. 1. Images of the endoluminal surface produced from the conformal mapping technique (case 11). The colour scheme shows the Shape Index (SI) and the vectors show the displacements generated from the landmark registration. Images show: a) the source (prone) image; b) the ambiguous vector direction on the source image; c) the sorted displacements; d) the source image vertically aligned to reduce displacements; e) the source image with displacement vectors and regular grid; f) the result of the landmark B-spline registration with transformed image and grid; g) the refinement with the intensity based registration (with same grid); h) the target (supine) image.

3 Evaluation

3.1 Data

Ethical approval and informed consent was obtained to use anonymised CT colonography data. Colonic cleansing and insufflations has been performed in accordance with current recommendations [11]. These data consist of 17 validation cases of which 5 exhibited local luminal collapse (see table 1), and 4 cases (cases 9 - 12) that had been excluded from a previous study using an intensity based registration [7] due to marked differences in local distension and therefore different surface features. Cases used fluid tagging (allowing for digital cleansing of residual fluid) or little fluid remained. All parameters were optimised on separate training data. A radiologist (experienced in over 400 validated colonography studies) manually identified the centres of corresponding haustral folds using 'virtual colonoscopy' fly-through renderings, and external views of the colonic lumen. This resulted in 1484 pairs of corresponding positions between the two views to be used for evaluation.

Table 1. Information of cases exhibiting local luminal collapse. For each case, the number of collapsed regions in the prone and supine images are displayed, along with the Euclidean distance across each region. Locations of collapse are given (DC: descending colon; SC: sigmoid colon).

	Prone			Supine		
Case No.	Collapses	Location	Distance (mm)	No. Collapses	Location	Distance (mm)
13	1	DC	65.0	0	-	-
14	1	DC	245.1	1	DC	272.4
15	0	-	-	1	SC	26.0
16	3	DC	6.5	0	-	-
		DC	34.4		-	-
		SC	8.0		-	-
17	0	-	-	1	DC	18.3

To assess the performance of each algorithm in terms of registration error, each reference standard point is transformed from prone to supine using the calculated transformation function and the 3D Euclidean distance between this and the corresponding reference standard point is measured. It is clear that the composite method outperforms both the intensity- and landmark-based registration methods at $7.0mm(\pm 2.7mm)$, compared to $12.1mm(\pm 10.6mm)$ and $9.2mm(\pm 3.4mm)$ respectively. Using a Related Samples Wilcoxon Signed Rank Test, the difference in error between each pair of results is statistically significant with $p < 0.001$.

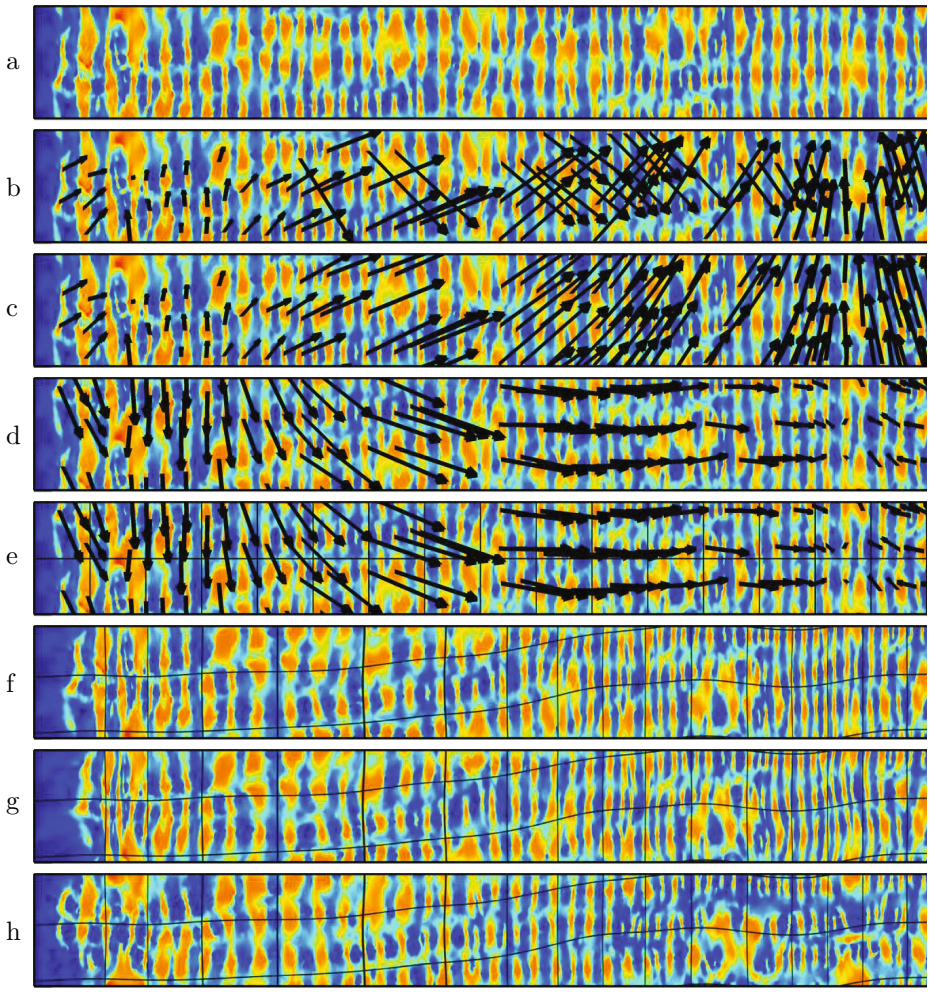

Fig. 2. Displaying the images in figure 1 in greater detail at the end of the colon. The colour scheme shows the Shape Index (SI) and the vectors show the displacements generated from the landmark registration. Images show: a) the source (prone) image, b) the ambiguous vector direction on the source image; c) the sorted displacements; d) the source image vertically aligned to reduce displacements; e) the source image with displacement vectors and regular grid; f) the result of the landmark B-spline registration with transformed image and grid; g) the refinement with the intensity based registration (with same grid); h) the target (supine) image.

Table 2. Mean fold registration error (mm) for each of the validation cases. Results are shown individually for the intensity, landmark and composite registration methods.

	Case	Intensity	Landmark	Composite
Fully Distended	1	12.0	10.1	11.7
	2	7.4	7.3	5.6
	3	5.3	6.0	5.2
	4	9.0	6.1	5.6
	5	5.6	5.1	5.6
	6	3.5	4.7	3.6
	7	5.9	6.4	5.6
	8	6.9	7.3	6.2
	Subset Mean	**7.0**	**6.6**	**6.2**
	Subset Std	**2.6**	**1.7**	**2.4**
	Previously Excluded Cases			
	9	44.9	15.2	5.8
	10	12.5	8.5	7.8
	11	16.8	10.3	6.0
	12	7.3	10.3	6.2
	Subset Mean	**20.4**	**11.1**	**6.5**
	Subset Std	**16.8**	**2.9**	**0.9**
Collapsed	13	30.3	16.2	15.0
	14	5.9	13.6	6.8
	15	7.5	11.1	7.2
	16	15.7	9.1	6.7
	17	8.8	8.4	7.6
	Subset Mean	**13.7**	**11.7**	**8.7**
	Subset Std	**10.0**	**3.2**	**3.6**
	Total Mean	**12.1**	**9.2**	**7.0**
	Total Std	**10.6**	**3.4**	**2.7**

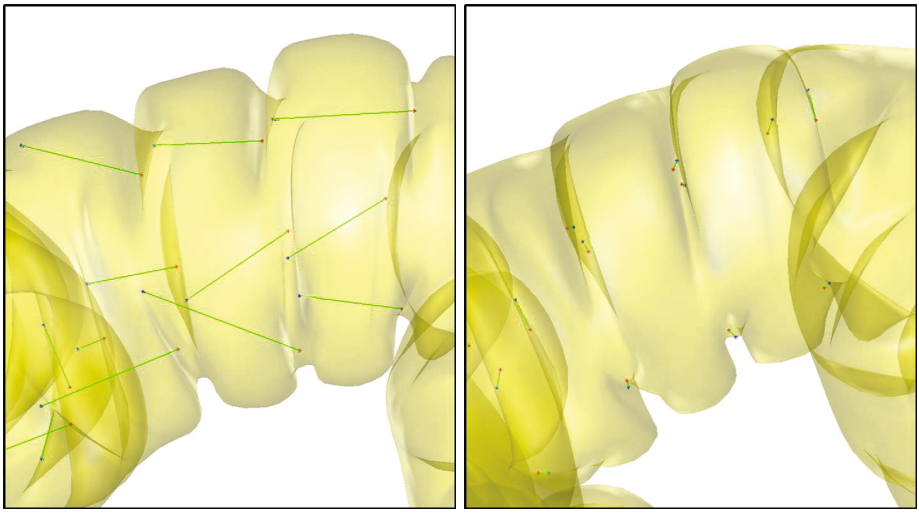

Fig. 3. External surface renderings of the transverse colon in the supine image of case 16. The set of reference standard points in the supine view (red) and the corresponding points transformed from the prone view (blue) and shown using the results from the intensity based (left) and composite (right) registration methods. The green lines show the Euclidean distance error.

4 Conclusion

Our composite registration method combines landmark and intensity based registration techniques and improves the mean registration accuracy compared to using either method alone. The work flow presented is fully automated, taking as input a prone and supine colon lumen segmentation. The consistency of results across cases showing a variety of characteristics indicates that the composite method will provide a more robust registration than those previously reported, especially in more 'difficult' cases, such as those that show marked differences in distension, or exhibit areas of local colonic collapse. This situation is very common in routine practice and therefore an algorithm that is robust to these characteristics is of greater clinical benefit.

References

1. Fukano, E., Oda, M., Kitasaka, T., Suenaga, Y., Takayama, T., Takabatake, H., Mori, M., Natori, H., Nawano, S., Mori, K.: Haustral fold registration in CT colonography and its application to registration of virtual stretched view of the colon. In: Proceedings of SPIE, vol. 7624, p. 762420 (2010)
2. Hampshire, T., Roth, H., Hu, M., Boone, D., Slabaugh, G., Punwani, S., Halligan, S., Hawkes, D.: Automatic Prone to Supine Haustral Fold Matching in CT Colonography Using a Markov Random Field Model. In: Fichtinger, G., Martel, A., Peters, T. (eds.) MICCAI 2011, Part I. LNCS, vol. 6891, pp. 508–515. Springer, Heidelberg (2011)

3. Jin, M., Kim, J., Luo, F., Gu, X.: Discrete surface ricci flow. IEEE Transactions on Visualization and Computer Graphics 14(5), 1030–1043 (2008)
4. Koenderink, J.J.: Solid shape. MIT Press, Cambridge (1990)
5. Lee, S., Wolberg, G., Shin, S.Y.: Scattered data interpolation with multilevel B-splines. IEEE Transactions on Visualization and Computer Graphics 3(3), 228–244 (1997)
6. Näppi, J., Okamura, A., Frimmel, H., Dachman, A., Yoshida, H.: Region-based supine-prone correspondence for the reduction of false-positive CAD polyp candidates in CT colonography. Academic Radiology 12(6), 695–707 (2005)
7. Roth, H., McClelland, J., Boone, B., Modat, M., Cardoso, M., Hampshire, T., Hu, M., Punwani, S., Ourselin, S., Slabaugh, G., Halligan, S., Hawkes, D.: Registration of the endoluminal surfaces of the colon derived from prone and supine CT colonography. Medical Physics 38(6), 3077–3089 (2011), http://link.aip.org/link/?MPH/38/3077/1
8. Rueckert, D., Sonoda, L.I., Hayes, C., Hill, D.L.G., Leach, M.O., Hawkes, D.J.: Nonrigid registration using free-form deformations: application to breast MR images. IEEE Transactions on Medical Imaging 18(8), 712–721 (1999)
9. Suh, J.W., Wyatt, C.L.: Deformable registration of supine and prone colons for computed tomographic colonography. Journal of Computer Assisted Tomography 33(6), 902 (2009)
10. Taylor, S.A., Halligan, S., Goh, V., Morley, S., Bassett, P., Atkin, W., Bartram, C.I.: Optimizing colonic distention for multi–detector row CT colonography: Effect of hyoscine butylbromide and rectal balloon catheter. Radiology 229(1), 99 (2003)
11. Taylor, S.A., Laghi, A., Lefere, P., Halligan, S., Stoker, J.: European society of gastrointestinal and abdominal radiology (esgar): consensus statement on CT colonography. European Radiology 17(2), 575–579 (2007)
12. Wang, S., Yao, J., Liu, J., Petrick, N., Van Uitert, R.L., Periaswamy, S., Summers, R.M.: Registration of prone and supine CT colonography scans using correlation optimized warping and canonical correlation analysis. Medical Physics 36, 5595 (2009)
13. Weiss, Y., Freeman, W.T.: On the optimality of solutions of the max-product belief-propagation algorithm in arbitrary graphs. IEEE Transactions on Information Theory 47(2), 736–744 (2002)
14. Zeng, W., Marino, J., Gurijala, K.C., Gu, X., Kaufman, A.: Supine and prone colon registration using quasi-conformal mapping. IEEE Transactions on Visualization and Computer Graphics 16, 1348–1357 (2010)
15. Zeng, W., Samaras, D., Gu, D.: Ricci flow for 3D shape analysis. IEEE Transactions on Pattern Analysis and Machine Intelligence 32(4), 662–677 (2010)